Tokunaga, F., Iwasa, T., & Yoshizawa, T. (1976) *FEBS Lett. 72,* 33–38.
Trissl, H.-W. (1983) *Biochim. Biophys. Acta 723,* 327–331.
Trissl, H.-W. (1985) *Biochim. Biophys. Acta 806,* 124–135.
Warshel, A. (1979) *Photochem. Photobiol. 30,* 285–290.
Zinth, W., Nuss, M. C., Polland, H. J., Franz, M. A., & Kaiser, W. (1985) in *Spectroscopy of Biological Molecules* (Alix, A. J. P., Bernard, L., & Manfait, M., Eds.) pp 325–331, Wiley, Chichester, New York, Brisbane, Toronto, and Singapore.

Laser Flash Photolysis Studies of Electron Transfer between Ferredoxin–NADP$^+$ Reductase and Several High-Potential Redox Proteins†

Anjan K. Bhattacharyya, Terrance E. Meyer, Michael A. Cusanovich, and Gordon Tollin*
Department of Biochemistry, University of Arizona, Tucson, Arizona 85721

Received April 29, 1986; Revised Manuscript Received October 1, 1986

ABSTRACT: Complex formation and the kinetics of electron transfer between ferredoxin–NADP$^+$ reductase (FNR) and two structurally homologous acidic 4Fe–4S high-potential ferredoxins (HiPIP's) from *Ectothiorhodospira halophila* (HP1 and HP2) and two structurally homologous cytochromes c_2 from *Paracoccus denitrificans* and *Rhodospirillum rubrum* (PC2, and RC2, respectively) have been investigated by gel filtration and laser flash photolysis techniques. Gel filtration studies indicated that complex formation occurred between $\mathrm{FNR_{ox}}$ and $\mathrm{HP1_{ox}}$ or $\mathrm{HP2_{ox}}$ at low ionic strength (10 mM) and that the complexes were completely dissociated at high ionic strength (310 mM). Laser flash photolysis using lumiflavin as the reductant demonstrated that both free $\mathrm{HP1_{ox}}$ and $\mathrm{HP2_{ox}}$ reacted primarily with the anionic form of fully reduced lumiflavin ($\mathrm{LFH^-}$), whereas FNR was unreactive. Second-order rate constants of 1×10^6 and 0.8×10^6 $\mathrm{M^{-1}\ s^{-1}}$ were obtained for these reactions at 10 mM ionic strength. Increasing the ionic strength to 310 mM resulted in an approximately 1.5-fold increase in the rate constant. Inclusion of stoichiometric amounts of $\mathrm{FNR_{ox}}$ into the reaction mixture at low ionic strength led to a 2.5-fold increase in the rate constants. The reaction of 5-deazariboflavin semiquinone (5-dRf·) with the oxidized HiPIP's was also investigated by laser flash photolysis. Second-order rate constants of 3.0×10^8 $\mathrm{M^{-1}\ s^{-1}}$ (HP1) and 2.5×10^8 $\mathrm{M^{-1}\ s^{-1}}$ (HP2) were obtained for the free proteins at 10 mM ionic strength. Under the same conditions, 5-dRf· reacted with free $\mathrm{FNR_{ox}}$, resulting in the formation of the neutral protein-bound semiquinone (FNR·), with a second-order rate constant of 6×10^8 $\mathrm{M^{-1}\ s^{-1}}$. The reduction kinetics of 1:1 $\mathrm{FNR_{ox}}$–$\mathrm{HiPIP_{ox}}$ complexes at $I = 10$ mM were also investigated. In the case of the $\mathrm{FNR_{ox}}$–$\mathrm{HP1_{ox}}$ complex, reduction by 5-dRf· led to the initial rapid formation of both FNR· and $\mathrm{HP1_{red}}$. A subsequent, slower intracomplex electron-transfer reaction from FNR· to $\mathrm{HP1_{ox}}$ was observed to occur with a first-order rate constant of 23 $\mathrm{s^{-1}}$. The reduction kinetics of the $\mathrm{FNR_{ox}}$–$\mathrm{HP2_{ox}}$ complex using 5-dRf· were similar to those of the $\mathrm{FNR_{ox}}$–$\mathrm{HP1_{ox}}$ complex. However, the limiting first-order rate constant corresponding to the intracomplex reaction between FNR· and $\mathrm{HP2_{ox}}$ was much smaller ($k = 4$ $\mathrm{s^{-1}}$). Gel filtration experiments indicated that complex formation between $\mathrm{FNR_{ox}}$ and $\mathrm{PC2_{ox}}$ or $\mathrm{RC2_{ox}}$ occurred at low ionic strength (10 mM) and dissociation was observed at high ionic strength (310 mM). Lumiflavin semiquinone (LfH·) reacted with both cytochromes, and second-order rate constants of 5.5×10^7 and 7.9×10^7 $\mathrm{M^{-1}\ s^{-1}}$ were obtained with $\mathrm{PC2_{ox}}$ and $\mathrm{RC2_{ox}}$, respectively. The reactivity of the cytochromes with LfH· within the complex, i.e., in the presence of stoichiometric amounts of $\mathrm{FNR_{ox}}$ at low ionic strength, remained unchanged, suggesting that access of LfH· to the heme was not influenced by the presence of FNR. The 5-dRf· reaction with the oxidized free cytochromes gave second-order rate constants of 6×10^8 and 9×10^8 $\mathrm{M^{-1}\ s^{-1}}$ for $\mathrm{PC2_{ox}}$ and $\mathrm{RC2_{ox}}$ at $I = 10$ mM. The 5-dRf· reaction at low ionic strength (10 mM) with the 1:1 $\mathrm{FNR_{ox}}$ complexes with both cytochromes resulted in the initial rapid formation of both reduced cytochrome and FNR·. This was followed by a slower first-order intracomplex electron transfer from FNR· to the oxidized cytochromes. First-order rate constants of ~700 and ~400 $\mathrm{s^{-1}}$ were obtained for $\mathrm{PC2_{ox}}$ and $\mathrm{RC2_{ox}}$, respectively. At high ionic strength, the reaction of FNR· with oxidized $\mathrm{PC2_{ox}}$ was second order ($k = 5 \times 10^6$ $\mathrm{M^{-1}\ s^{-1}}$), consistent with the observed dissociation of the complex. The results of these experiments are interpreted in terms of possible structural features of the complexes formed between FNR and the redox protein electron acceptors. The physiological FNR–Fd complex is the only one in which access to the electron-transfer site is diminished, probably because it is located within the protein–protein interaction domain. The intracomplex electron-transfer reactions within the nonphysiological complexes are slower than expected on the basis of the thermodynamic driving force (redox potential difference), most likely as a result of nonoptimal orientations between redox centers, and larger distances over which electron transfer must occur.

In previous work from this laboratory, we have reported on the kinetics of electron-transfer reactions between various physiological and nonphysiological donors and acceptors in an attempt to elucidate the factors involved in determining the rates of electron transfer to and within electrostatically stabilized protein–protein complexes (Przysiecki et al., 1985; Bhattacharyya et al., 1986; Ahmad et al., 1982; Simondsen

---

† This work was supported in part by NIH Grants AM 15057 (to G.T.) and GM 21277 (to M.A.C.).

0006-2960/87/0426-0758$01.50/0 © 1987 American Chemical Society

et al., 1982; Simondsen & Tollin, 1983; Hazzard & Tollin, 1985; Hazzard et al., 1986). The occurrence of rapid intracomplex electron transfer between Fd_{red}[1] and FNR_{ox} (Bhattacharyya et al., 1986) and between the neutral semiquinone of FNR and oxidized *Clostridium pasteurianum* rubredoxin (Przysiecki et al., 1985) has been demonstrated. The first-order rate constants for these reactions did not correlate with the differences in one-electron redox potential between the reactants, and thus primarily reflected the influence of structural parameters. In the present work, we have extended these studies to include complex formation and electron transfer between FNR and several structurally homologous acidic HiPIP's and cytochromes. Each of the systems described in this paper has a larger driving force (i.e., difference in one-electron redox potential) between the components than does either of the previously studied FNR complexes. Furthermore, the HiPIP's and cytochromes which were investigated have different net charges at neutral pH. Thus, the effects of both electrostatic interactions and redox potential differences can be assessed.

We have used gel filtration and laser flash photolysis methods (Tollin et al., 1982; Cusanovich & Tollin, 1980; Bhattacharyya et al., 1983, 1986; Cusanovich et al., 1985) to characterize complex formation and electron-transfer kinetics. Lumiflavin was used as a reductant ($E_{m,7} = -238$ mV for the semiquinone form and $E_{m,7} = -167$ mV for the fully reduced species; neither of these is measurably reactive with FNR_{ox}) to probe the effect of complex formation with FNR on the accessibility of the redox centers of the oxidized HiPIP's and cytochromes. We have also determined the first-order rate constants for electron transfer from FNR· [produced by laser photolysis using 5-dRf· as a reductant ($E_{m,7} = -650$ mV)] to each electron acceptor within their respective complexes. The results provide some interesting insights into the effects of structure on the redox properties of these systems.

MATERIALS AND METHODS

Spinach FNR was purified by the method of Zanetti and Curti (1980). An extinction coefficient of 10.3×10^3 M^{-1} cm^{-1} at 458 nm was used to determine the oxidized FNR concentrations. High-potential ferredoxins (iso-1 and iso-2 HiPIP's) from *Ectothiorhodospira halophila* were isolated by the method of Meyer (1985). An extinction coefficient of 20×10^3 M^{-1} cm^{-1} at 385 nm was used to determine the concentration of the oxidized HiPIP's. Cytochromes c_2 from *Paracoccus denitrificans* and *Rhodospirillum rubrum* were isolated by the methods of Ambler et al. (1981) and Bartsch (1971). An extinction coefficient of 30×10^3 M^{-1} cm^{-1} at 550 nm for the reduced cytochromes was used to determine their concentrations. All buffer components were A.C.S. reagent grade. The buffer used for the low ionic strength experiments (10 mM) was 4 mM potassium phosphate–0.5 mM ethylenediaminetetraacetate (EDTA) and contained 100 μM 5-deazariboflavin (or 50 μM lumiflavin). Solid potassium chloride was used to adjust the buffer to the higher ionic strength (310 mM). All experiments were performed at pH 7.0.

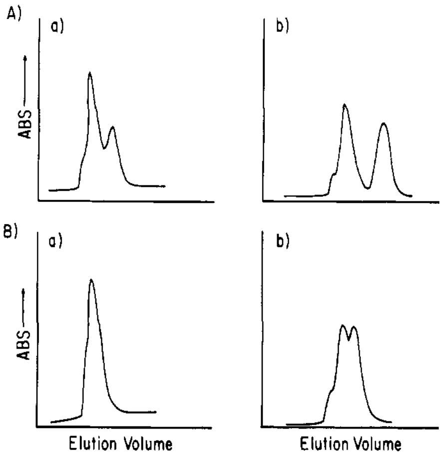

FIGURE 1: (A) Elution profiles of a 1:1 mixture of FNR_{ox}–$HP1_{ox}$ on Sephadex G-50 at ionic strengths of (a) 10 mM and (b) 310 mM. In each case, ~0.1 μmol of complex was loaded on the column. (B) Elution profiles of a 1:1 mixture of FNR_{ox}–$PC2_{ox}$ at (a) 10 mM and (b) 310 mM. In each case, 0.08 μmol of the complex was loaded on the column. The composition of the buffers and a description of the column are given under Materials and Methods.

Gel filtration experiments were carried out on a 1 × 25 cm Sephadex G-50 (superfine) column equilibrated with the appropriate buffer, and the absorbance of the emerging fractions was monitored at 254 nm on an LKB 4700 UV monitor.

All kinetic experiments were carried out under pseudo-first-order conditions, in which the concentration of oxidized protein was in large excess over the amount of flavin reductant produced per laser flash (<0.7 μM). Unless quantitation was required, the number of flashes averaged per experiment varied. All kinetic traces were analyzed by hand fitting to a single-exponential curve. Experiments were carried out at room temperature (23–25 °C) under anaerobic conditions. Although the photochemical reaction which generates the flavin reductant also produces oxidized species derived from EDTA, in this study as in all of our previous work, no kinetic complications were observed which could be attributed to these materials. A description of the laser flash photolysis apparatus and the method of data collection and analysis has been presented elsewhere (Przysiecki et al., 1985; Bhattacharyya et al., 1983).

RESULTS AND DISCUSSION

HIPIP's

Complex Formation with FNR. Complex formation between FNR_{ox} and the high-potential ferredoxins from *E. halophila* was investigated by using visible difference absorption spectroscopy and gel filtration techniques. Unlike the other negatively charged proteins which interact with FNR (Foust et al., 1969), no difference in the visible absorption spectrum could be detected between 1:1 protein mixtures at low (10 mM) and high (310 mM) ionic strengths. Gel filtration studies, however, demonstrated the occurrence of an alteration of the elution pattern at the higher ionic strength and that the proteins were predominantly dissociated at the higher ionic strength (Figure 1A). This is consistent with complex formation. No significant differences could be detected in the elution patterns of the 1:1 FNR_{ox}–$HP1_{ox}$ and FNR_{ox}–$HP2_{ox}$ mixtures at low and high ionic strengths, indicating that the two complexes are probably similar in stability. The dissociation of the protein complexes at the higher ionic strength

---

[1] Abbreviations: HiPIP, high-potential ferredoxin; FNR_{ox}, oxidized ferredoxin–NADP⁺ reductase; FNR·, neutral semiquinone of ferredoxin–NADP⁺ reductase; LF, lumiflavin; LfH·, lumiflavin semiquinone; LFH^-, anionic form of fully reduced lumiflavin; 5-dRf, 5-deazariboflavin; 5-dRf·, 5-deazariboflavin semiquinone; $HP1_{ox}$, oxidized iso-1 HiPIP from *Ectothiorhodospira halophila*; $HP1_{red}$, reduced iso-1 HiPIP from *E. halophila*; $HP2_{ox}$, oxidized iso-2 HiPIP from *E. halophila*; $HP2_{red}$, reduced iso-2 HiPIP from *E. halophila*; $PC2_{ox}$, oxidized cytochrome c_2 from *Paracoccus denitrificans*; $PC2_{red}$, reduced cytochrome c_2 from *P. denitrificans*; $RC2_{ox}$, oxidized cytochrome c_2 from *Rhodospirillum rubrum*; $RC2_{red}$, reduced cytochrome c_2 from *R. rubrum*; Fd, spinach 2Fe–2S ferredoxin; Rd, rubredoxin; EDTA, ethylenediaminetetraacetic acid.

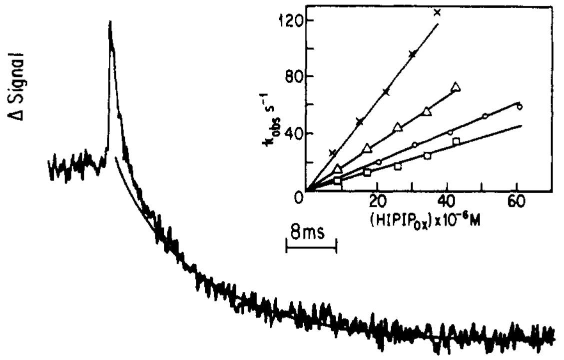

FIGURE 2: Reduction kinetics of $HP1_{ox}$ monitored at 560 nm with LFH^- as the reductant. The protein concentration was 70 μM, and lumiflavin concentration was 50 μM. The solid line is a single-exponential fit to the data. The inset shows second-order plots of reactions of LFH^- with (○) $HP1_{ox}$ and (□) $HP2_{ox}$ at 10 mM ionic strength and (×) $HP1_{ox}$ and (△) $HP2_{ox}$ at 310 mM ionic strength.

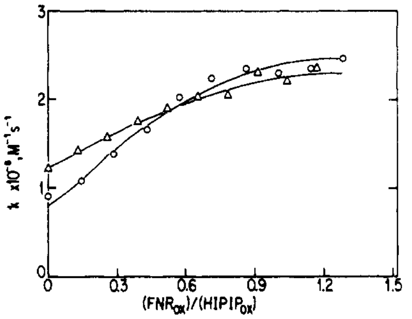

FIGURE 3: Dependence of the second-order rate constant for the reaction between LFH^- and oxidized HIPIP's on the addition of increasing amounts of FNR_{ox} at $I = 10$ mM for (△) $HP1_{ox}$ and (○) $HP2_{ox}$.

indicates that an attractive electrostatic interaction must influence complex formation.

Lumiflavin Semiquinone Reduction Kinetics of the Individual Components. Upon laser flash photolysis of lumiflavin in the presence of $HP1_{ox}$, a rapid increase in absorbance at 560 nm was observed, followed by a biphasic decrease which went below the preflash base line (Figure 2). These absorbance changes correspond to rapid formation (initial rise) of LfH·, disproportionation (initial fast decay) to form fully reduced lumiflavin (LFH^-), and the subsequent reaction of LFH^- with $HP1_{ox}$ (slower decay). Since the pK_a of fully reduced lumiflavin has been estimated to be approximately 6.0 (Draper & Ingraham, 1968), the anionic form (LFH^-) would be the predominant species present at pH 7.0, although it is quite likely that reaction can also occur with the LFH_2 form. A plot of k_{obsd} vs. $HP1_{ox}$ concentration yielded a second-order rate constant of 1×10^6 M^{-1} s^{-1} at $I = 10$ mM (inset, Figure 2). The reaction of laser-photoreduced lumiflavin with $HP2_{ox}$ yielded similar results with a second-order rate constant for LFH^- reduction of 0.8×10^6 M^{-1} s^{-1} (inset, Figure 2). For both proteins, the rate constants for the LFH· reactions were too small to be accurately measured due to the competing disproportionation reaction.

Since both of the reactants (LFH^- and HiPIP) in the above-mentioned electron transfer are negatively charged, increasing the ionic strength should result in an increase in the second-order rate constant. The data in Figure 2 (inset) show that this is indeed the case, inasmuch as when the ionic strength was increased from 10 to 310 mM, the second-order rate constants for the reactions of both $HP1_{ox}$ and $HP2_{ox}$ with LFH^- increased by approximately 2–3-fold. This is consistent with a weaking of the repulsive electrostatic forces between the two negatively charged species.

Fully Reduced Lumiflavin Reduction Kinetics of the 1:1 FNR–HiPIP$_{ox}$ Complexes at Low Ionic Strength. In order to investigate the kinetics of reduction of the oxidized HiPIP's in the presence of FNR_{ox} at low ionic strength, under which conditions complex formation should occur, we performed experiments in which increasing substoichiometric amounts of FNR_{ox} were added to a 10 mM ionic strength solution containing oxidized HiPIP and lumiflavin. Upon flash photolysis (monitored at 560 nm), LFH^- reduction of the oxidized HiPIP was observed, and as the FNR_{ox} concentration was increased, the apparent second-order rate constant for the LFH^- reaction also increased (Figure 3). At FNR_{ox}:$HiPIP_{ox}$ ratios approaching unity, the kinetics became relatively independent of the concentration of added FNR_{ox}. These results demonstrate that both HiPIP species remained easily reducible within the complex and that in both cases an approximately 2.5-fold increase in the second-order rate constant for HiPIP reduction by LFH^- was observed upon complexation with FNR_{ox}. This increase in rate constant can be attributed either to a change in the HiPIP redox potential or conformation upon complex formation or to a decreased repulsive interaction between LFH^- and the oxidized HiPIP in the complex resulting from charge cancellation effects between the negatively charged HiPIP and the positively charged binding site on the oxidized FNR molecule. This needs further investigation when the FNR structure is available. The results also indicate that the stoichiometry of the complexes is 1:1, since the observed rate constants became relatively independent of FNR_{ox} concentrations at protein ratios above unity.

We also performed experiments in which increasing amounts of a 1:1 FNR_{ox}–$HiPIP_{ox}$ mixture were added to a low ionic strength solution containing Lf. As expected, reduction of $HiPIP_{ox}$ was observed, and plots of k_{obsd} vs. complex concentration yielded second-order rate constants of 3×10^6 and 2.5×10^6 M^{-1} s^{-1} for the FNR_{ox}–$HP1_{ox}$ and FNR_{ox}–$HP2_{ox}$ complexes, respectively (data not shown). These results are in reasonable agreement with the results of the titration experiments in which limiting second-order rate constants of ~2.5×10^6 M^{-1} s^{-1} were obtained for both systems (Figure 3).

5-Deazariboflavin Semiquinone Reduction Kinetics of the Free Oxidized HiPIP's. We have previously reported on the 5-dRf· reaction with FNR_{ox} ($k = 6 \times 10^8$ M^{-1} s^{-1}) which leads to the formation of FNR· (Przysiecki et al., 1985). The reaction of 5-dRF· with free $HP1_{ox}$ and $HP2_{ox}$ was followed at 500 nm. Upon laser flash photolysis in the presence of the oxidized HiPIP, a rapid absorbance increase was observed followed by a single-exponential decay that eventually went below the preflash base line (data not shown). This latter result is consistent with rapid formation and reoxidation of 5-dRf·, concomitant with reduction of the oxidized HiPIP. Second-order rate constants of 2.5×10^8 and 2.0×10^8 M^{-1} s^{-1} at $I = 10$ mM were obtained for the reactions between 5-dRf· and $HP1_{ox}$ and $HP2_{ox}$, respectively.

5-Deazariboflavin Semiquinone Reduction Kinetics of the 1:1 FNR–HiPIP$_{ox}$ Complexes. On the basis of the reported one-electron redox potentials of FNR ($E_{m,7} = -320$ mV), $HP1_{ox}$ ($E_{m,7} = 120$ mV), and $HP2_{ox}$ ($E_{m,7} = 50$ mV) (Keirns & Wang, 1972; Meyer et al., 1983), it is expected that the predominant direction of intracomplex electron transfer would be from the semiquinone of FNR to the oxidized HiPIP's. On the basis of results of the lumiflavin experiments, it is also expected that the bound HiPIP's can be directly reduced within the complex by 5-dRf·. In order to determine the sequence of events occurring upon 5-dRf· interaction with the complex,

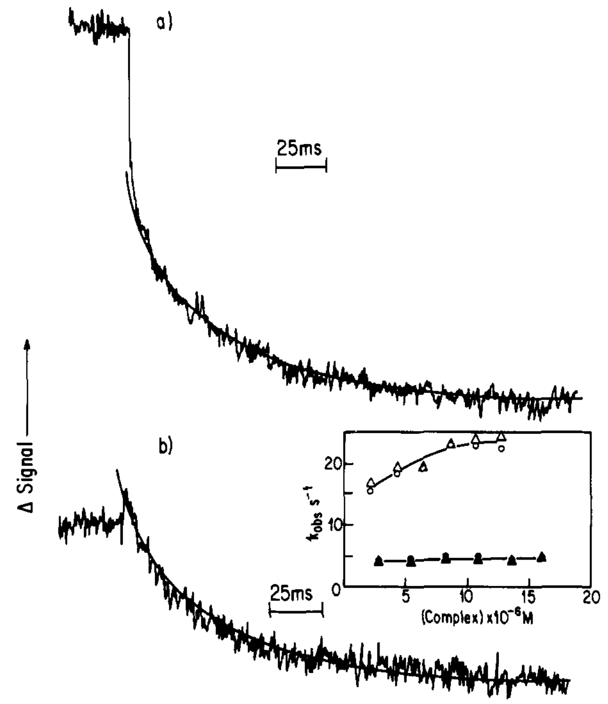

FIGURE 4: (a) Biphasic reduction on HP1$_{ox}$ by 5-dRf·, monitored at 500 nm, in the 1:1 FNR$_{ox}$–HP1$_{ox}$ complex at low ionic strength upon laser flash photolysis. The complex concentration was 15 μM. The solid line is a single-exponential fit to the slower decay. (b) Slow reoxidation of FNR· by HP1$_{ox}$ in the 1:1 FNR$_{ox}$–HP1$_{ox}$ complex, monitored at 590 nm. The solid line is a single-exponential fit to the data. The inset shows the dependence of the rate constants of the slow phase on the concentration of the oxidized complexes: FNR$_{ox}$–HP1$_{ox}$, (△) 500 nm and (○) 590 nm; FNR$_{ox}$–HP2$_{ox}$, (▲) 500 nm and (●) 590 nm.

we added increasing amounts of a 1:1 mixture of FNR$_{ox}$ and oxidized HiPIP to a 10 mM ionic strength solution containing 5-dRf. Upon flash photolysis (monitored at 500 nm, which is an approximate isosbestic point for FNR), an initial rapid decrease in absorbance was observed, followed by a much slower exponential absorbance decrease (Figure 4a). These changes are consistent with rapid direct reduction of HP1$_{ox}$ by 5-dRf· (fast decrease) and a subsequent slower reduction of HP1$_{ox}$ (slow decrease). This latter process had a k_{obsd} of 23 s^{-1}. In order to confirm the nature of the slower reaction, we followed the reduction kinetics at 590 nm, a wavelength at which the absorbance change due to HP1$_{ox}$ reduction is small and that due to FNR· oxidation is large. Furthermore, at this wavelength the absorbance changes in the fast phase of the reaction tend to cancel one another and in the slow phase tend to reinforce each other. The results show that the predominant transient observed was a slow decrease in absorbance that began slightly above the preflash base line (Figure 4b). The first-order rate constant obtained for this slow process (23 s^{-1}) was the same as or the slow absorbance decrease observed at 500 nm (Figure 4a). The results of Figure 4b are consistent with the rapid formation and slower reoxidation of FNR·, leading to the formation of HP1$_{red}$.

Time-resolved flash-induced difference spectra (Figure 5) for the FNR$_{ox}$–HP1$_{ox}$ system, obtained at t = 0 ms (extrapolated) and t = 250 ms following the laser flash, are consistent with initial direct reduction of some of the FNR$_{ox}$ to FNR· and of the HP1$_{ox}$ to HP1$_{red}$ followed by a slower electron transfer from FNR· to some of the remaining oxidized HiPIP. The solid line drawn through the data points represented by the closed circles (t = 0 ms) corresponds to a calculated difference spectrum comprised of both FNR· and HP1$_{red}$ and thus represents the initial direct reduction of FNR$_{ox}$ and HP1$_{ox}$ by 5-dRf·. The agreement between this spectrum and the flash data is quite good. The solid line drawn through the data represented by the closed triangles (t = 250 ms) corresponds to a reduced minus oxidized difference spectrum obtained by dithionite reduction of HP1$_{ox}$ in a spectrophotometer. Again, the agreement is satisfactory, and thus at 250 ms essentially all the FNR· had reacted with the remaining HP1$_{ox}$ to form HP1$_{red}$.

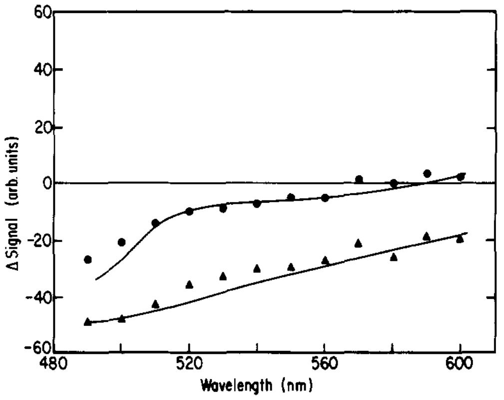

FIGURE 5: Laser flash induced time-resolved difference spectra (oxidized minus reduced) for the reactions shown in Figure 4. (●) t = 0 ms (extrapolated); (▲) t = 250 ms. The solid line drawn through the closed circles represents the sum of the difference spectra of FNR· and HP1$_{red}$. The solid line drawn through the closed triangles corresponds to an oxidized minus reduced HP1$_{ox}$ spectrum obtained by dithionite reduction in a spectrophotometer.

In order to determine whether the slow electron-transfer reaction occurred within the complex (i.e., was kinetically first order), we increased the concentration of the 1:1 mixture of the oxidized proteins. The plot of k_{obsd} vs. protein concentration shown in the inset of Figure 4 indicates that, over the accessible range of concentrations, the rate constant of the reaction corresponding to electron transfer from FNR· to HP1$_{ox}$ (i.e., the slow phase) became independent of concentration, consistent with a first-order intracomplex reaction. A limiting first-order rate constant of ~23 s^{-1} was obtained for electron transfer from FNR· to HP1$_{ox}$ within the complex. The lower k_{obsd} values obtained at the smaller protein concentrations probably resulted from the parallel second-order reaction which occurred between dissociated FNR· and HP1$_{ox}$.

When the same experiments were carried out with the FNR$_{ox}$–HP2$_{ox}$ complex, a limiting rate constant of ~4 s^{-1} was obtained for the intracomplex electron transfer (Figure 4, inset). Once again, the kinetics were predominantly biphasic at 500 nm, whereas at 590 nm the slow reoxidation of FNR· and reduction of HP2$_{ox}$ were the principal processes observed (data not shown). The time-resolved flash-induced difference spectra obtained for the FNR$_{ox}$–HP2$_{ox}$ complex (measured at t = 0 and t = 1 s) were qualitatively similar to those obtained for the FNR$_{ox}$–HP1$_{ox}$ complex (data not shown).

Kinetic Studies at High Ionic Strength. The reduction kinetics of 1:1 mixtures of FNR$_{ox}$–HiPIP$_{ox}$ by 5-dRf· were also investigated at high ionic strength (310 mM). Upon flash photolysis of the FNR$_{ox}$–HP1$_{ox}$ (1:1) mixture monitored at 500 nm, an initial rapid absorbance decrease was observed followed by a much slower decrease (data not shown). Such absorbance changes are consistent with a rapid direct reduction of HP1$_{ox}$ by 5-dRf·, followed by a much slower additional reaction between FNR· and HP1$_{ox}$. In this case, however, the kinetics of the slow phase of reduction were second order (k = 6.2 × 10^5 M^{-1} s^{-1}; data not shown), consistent with the reduction of free HP1$_{ox}$ by free FNR·. This result was not unexpected since the complex is fully dissociated at this ionic strength. When the same experiment was performed on the FNR$_{ox}$–HP2$_{ox}$ system, again direct reduction of HP2$_{ox}$ by 5-dRf· was apparent (data not shown). However, under these conditions, FNR· was not measurably reactive with HP2$_{ox}$ (up to 5 s).

Cytochromes c_2

Complex Formation with FNR. Complex formation and the electron-transfer reactions between FNR$_{ox}$ and two structurally homologous cytochromes (*P. denitrificans* and *R. rubrum* cytochromes c_2) were also investigated by spectroscopic, gel filtration, and laser flash photolysis techniques. Visible absorption difference spectral measurements made at low (10 mM) and high (310 mM) ionic strengths for a 1:1 mixture of oxidized FNR and the cytochromes indicated that no significant perturbation of the spectra of either protein occurred upon mixing. Gel filtration experiments (on Sephadex G-50) (Figure 1B) showed that at low ionic strength (10 mM) in the presence of stoichiometric amounts of FNR$_{ox}$ both cytochromes eluted as a single peak, whereas dissociation occurred at the higher ionic strength (310 mM, Figure 1B). The dissociation of the complexes at higher ionic strength again indicates that an attractive electrostatic interaction must be involved in the formation of each complex. Both cytochromes are known to possess an asymmetric charge distribution with the negatively charged region located away from the heme edge and the positively charged surface dominating that portion of the cytochrome molecule which surrounds the exposed heme edge (Timkovich et al., 1976; Timkovich & Dickerson, 1979a,b; Salemme et al., 1973; Weber & Tollin, 1985; Dus et al., 1968). On the basis of electrostatics, FNR$_{ox}$ would be expected to bind to the negatively charged portion of each cytochrome, i.e., away from the exposed heme edge. Thus, intracomplex electron transfer might either be prevented or be slowed down by being forced to occur over large distances.

Lumiflavin Semiquinone Reduction Kinetics of the Individual Proteins. The reaction of the lumiflavin semiquinone generated by the laser flash with the two cytochromes was followed at 575 nm. At this wavelength, upon flash photolysis, an initial rapid increase in absorbance was observed followed by an exponential decay that eventually went below the preflash base line (data not shown). This is consistent with rapid formation and subsequent reoxidation of LfH· leading to the formation of reduced cytochrome. Plots of k_{obsd} vs. oxidized cytochrome concentration at $I = 10$ mM yielded second-order rate constants of 5.5×10^7 and 7.9×10^7 M^{-1} s^{-1} for PC2$_{ox}$ and RC2$_{ox}$ respectively. FNR$_{ox}$ was not measurably reactive with LfH· up to 50 μM protein concentration.

Lumiflavin Semiquinone Reduction Kinetics of the 1:1 FNR$_{ox}$–Cytochrome c_2 Complexes at Low Ionic Strength. In order to investigate the accessibility of the cytochrome heme within the complex, we measured the kinetics of reduction of the two cytochromes with LfH· in 1:1 FNR$_{ox}$–cyt$_{ox}$ mixtures at 10 mM ionic strength. Under these conditions, LfH· produced by the laser flash reacted in a second-order manner with both cytochromes within their respective complexes. Second-order rate constants of 4.3×10^7 and 8.6×10^7 M^{-1} s^{-1} were obtained for the reduction of the FNR$_{ox}$–PC2$_{ox}$ and FNR$_{ox}$–RC2$_{ox}$ complexes, respectively. Thus, the second-order rate constants remained essentially unchanged, indicating that the heme was as accessible to LfH· as in the free cytochrome (assuming that no significant change in redox potential occurred upon complexation). This result is consistent with the FNR molecule binding to the negatively charged sites of the two cytochromes, i.e., away from the heme edge.

5-Deazariboflavin Semiquinone Reduction Kinetics of the Individual Proteins. The reduction kinetics of the individual oxidized cytochromes by 5-dRf· (monitored at 500 nm) were investigated at low ionic strength (10 mM). 5-dRf· was rapidly reoxidized in a pseudo-first-order manner by the oxidized cytochromes (data not shown). Plots of k_{obsd} vs. oxidized protein concentrations yielded second-order rate constants of 6×10^8 and 9×10^8 M^{-1} s^{-1} for PC2$_{ox}$ and RC2$_{ox}$, respectively.

5-Deazariboflavin Semiquinone Reduction Kinetics of the FNR$_{ox}$–Cytochrome c_2 Complex at Low Ionic Strength. On the basis of the reported one-electron redox potentials of FNR$_{ox}$, PC2$_{ox}$, and RC2$_{ox}$ (−320, +250, and +340 mV; Keirns & Wang, 1972; Meyer et al., 1983; Pettigrew et al., 1978), one should observe irreversible intracomplex electron transfer from FNR· to the oxidized cytochromes c_2. In order to investigate this, we performed experiments in which increasing amounts of the preformed 1:1 FNR$_{ox}$–cytochrome $c_{2_{ox}}$ complex were added to a 10 mM ionic strength solution containing 5-dRf. The kinetic trace in Figure 6a, obtained upon flash photolysis monitored at 590 nm where FNR· absorbance should predominate, shows an initial rapid increase in absorbance, followed by an exponential decay that eventually went below the preflash base line. Such changes are consistent with formation and subsequent reoxidation of FNR·, leading to production of reduced heme (which has an absorbance decrease at 590 nm). With increasing complex concentration, the rate of FNR· reoxidation remained essentially constant (inset, Figure 6c), indicating that this was a first-order process. A limiting first-order rate constant of ~700 s^{-1} was obtained for intracomplex reduction of PC2$_{ox}$. Because of the small signal sizes obtained in these experiments, which was mainly a consequence of the large extent of direct cytochrome reduction in the complex, this value should be considered approximate. When the kinetics were monitored at 550 nm, a wavelength at which both FNR and heme undergo an increase in absorbance but at which heme predominates, an initial rapid rise due to direct cytochrome and FNR reduction followed by a slower increase was observed (Figure 6b). The first-order rate constant for the slow increase in absorbance was the same (within experimental uncertainty) as the rate constant for the slow reoxidation of FNR· and heme reduction observed at 590 nm. Once again, the rate constant for the slower increase in absorbance was independent of the complex concentration (inset, Figure 6c).

The flash-induced time-resolved (oxidized minus reduced) difference spectra shown in Figure 6c are consistent with an initial reduction of both the heme and FNR moieties ($t = 0$ ms, extrapolated values), and at $t = 10$ ms (when all kinetic processes were essentially complete) with the reoxidation of FNR· and the formation of additional reduced heme. The isosbestic points and relative peak heights again are not as well determined due to the large slit widths required for data collection. The direct reduction of PC2$_{ox}$ in the complex was expected, since the lumiflavin semiquinone kinetics indicated that the heme remained as accessible to reduction in the complex as in the free state, and the rate constants for 5-dRF· reduction of the individual components were comparable.

At high ionic strength, the reaction of flash-produced FNR· with PC2$_{ox}$ was second order ($k = 5 \times 10^6$ M^{-1} s^{-1}; data not shown). This is consistent with the lower complex stability under these conditions.

When the same experiments were performed on the FNR$_{ox}$–RC2$_{ox}$ complex at $I = 10$ mM, the reaction of 5-dRf· with the complex again resulted in the initial reduction of both

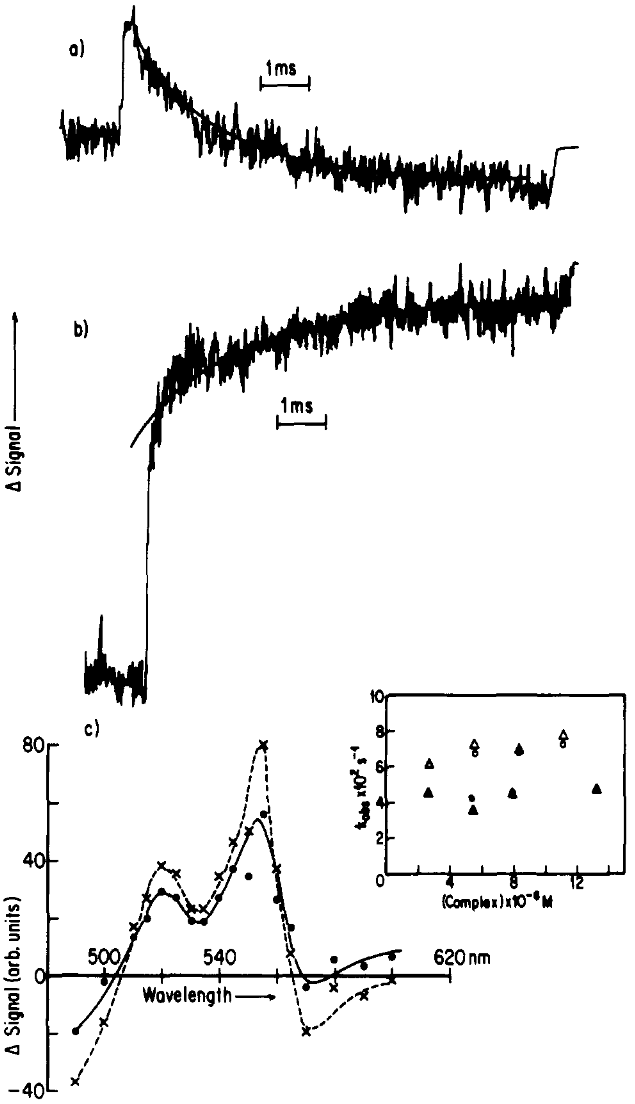

FIGURE 6: (a) Kinetic trace showing rapid formation and slower reoxidation of FNR· by $PC2_{ox}$ in the 1:1 FNR_{ox}–$PC2_{ox}$ complex leading to the formation of $PC2_{red}$. The reaction was monitored at 590 nm. The solid line is a single-exponential fit to the data. (b) Kinetic trace showing rapid direct reduction of $PC2_{ox}$ by 5-dRf· followed by slower reduction by FNR· in the 1:1 FNR_{ox}–$PC2_{ox}$ complex at 10 mM ionic strength. The reaction was monitored at 550 nm. The solid line is a single-exponential fit to the slow phase of the reaction. The protein concentration in (a) and (b) was 12 μM. The inset shows the dependence of the rate constants for the slow reactions on complex concentration for FNR_{ox}–$PC2_{ox}$ at (○) 590 nm and (△) 550 nm and for FNR_{ox}–$RC2_{ox}$ at (●) 590 nm and (▲) 550 nm. (c) Laser flash induced time-resolved difference spectra (oxidized minus reduced) obtained for the 1:1 FNR_{ox}–$PC2_{ox}$ complex at 10 mM ionic strength measured at (●) $t = 0$ ms (extrapolated) and (×) $t = 10$ ms following the laser flash. The protein concentration was the same as in (a) and (b).

RC2 and FNR, and FNR· was subsequently reoxidized by $RC2_{ox}$, leading to formation of additional $RC2_{red}$ (data not shown). A first-order rate constant of ~400 s^{-1} was obtained for electron transfer from FNR· to $RC2_{ox}$ within the complex (inset, Figure 6c). Again due to the poor signal to noise ratios in these experiments, this value is an approximation. The time-resolved flash-induced difference spectra at $t = 0$ ms (extrapolated) and $t = 15$ ms (when all kinetic processes were complete) were qualitatively similar to those obtained for the FNR_{ox}–$PC2_{ox}$ complex (data not shown).

Table I: First- and Second-Order Rate Constants for Electron-Transfer Reactions between FNR and Various Redox Proteins

reaction	k_1[a] (s^{-1})	k_2[b] (M^{-1} s^{-1})	$\Delta E_{m,7}$ (mV)
FNR_{ox} + Fd_{red}	>4 × 10^3	1.5 × 10^8	50
FNR· + Rd_{ox}	2.1 × 10^3	4 × 10^6	260
FNR· + $HP1_{ox}$	23	6.2 × 10^5	440
FNR· + $HP2_{ox}$	4	too slow to measure	370
FNR· + $PC2_{ox}$	~700[c]	5 × 10^6	570
FNR· + $RC2_{ox}$	~400[c]	not determined	660

[a] Rate constants measured at $I = 10$ mM, except for FNR_{ox} + Fd_{red}, for which the value is an estimate based on measurements obtained at high ionic strengths [cf. Bhattacharyya et al. (1986)]. [b] Rate constants measured at $I = 310$ mM. Although, in principle, it would be better to compare rate constant values extrapolated to infinite ionic strength so as to eliminate electrostatic effects, in our experience ionic strength dependencies tend to become relatively level at ionic strengths above 300 mM [cf. Tollin et al. (1984)]. [c] These values are approximate (see text).

CONCLUSIONS

The results presented above clearly demonstrate the occurrence of complex formation between FNR_{ox} and the acidic redox proteins studied, as well as intracomplex electron transfer from FNR· to the oxidized redox centers. Table I lists the first- and second-order rate constants obtained in this and the previous work (Przysiecki et al., 1985; Bhattacharyya et al., 1986). Although we are not dealing with a single structurally homologous series of redox proteins, it is clear that there is no consistent correlation between the redox potential differences between the participating electron-transfer centers and the observed rate constants of the various reactions. Furthermore, the largest values are obtained for the physiological FNR–Fd interactions, even though the thermodynamic driving force is the smallest for this system. We must conclude, therefore, that structural factors predominate (e.g., orientation and distance between redox centers).

It is important to note that, of the redox proteins listed in Table I, only Fd has its second-order rate constant for reduction diminished by complex formation with FNR (Bhattacharyya et al., 1986). Presumably, this is a consequence of steric factors, which implies that the iron–sulfur cluster points toward the FNR molecule within the complex, making it less accessible to external reductants. On the basis of the ionic strength dependence of the first-order rate constant for intracomplex electron transfer, we have previously argued that the electrostatic interactions between Fd and FNR serve to orient the redox centers in a manner favorable for reaction. In the case of the HiPIP's, the relatively uniform charge distribution over the surface of the protein molecule [based on sequence homology with the HiPIP from *Chromatium vinosum* whose three-dimensional structure is known; cf. Przysiecki et al. (1985)] suggests that a number of nonoptimal orientations of FNR and HiPIP could exist in intermediate complexes formed during the course of the reaction. Furthermore, the iron–sulfur cluster is in a relatively hydrophobic region of the HiPIP and is not well exposed to the solvent. Therefore, the slow rates of intracomplex electron transfer may be due to the relatively large average distance between the redox centers over which reaction must occur. In the event that a high-resolution X-ray crystal structure becomes available for FNR, one may be able to generate hypothetical complexes between FNR and the HiPIP's (using the *C. vinosum* structure) by the use of computer graphics (Simondsen et al., 1982; Weber & Tollin, 1985) in order to investigate specific structural features that may influence the electron-transfer rates.

As discussed previously, it is likely that the FNR molecule binds to the back side of the two cytochromes. On the basis of calculations using the crystallographic coordinates of each cytochrome, the distance of closest approach to the atoms of the pyrrole rings of the heme macrocycle (calculated from the carbon atoms of the residues closest to the tryptophan residue in the heme binding site) from this region of the structure is in the range of 9–11 Å. This is not an unreasonable distance over which tunneling could occur during the intracomplex electron-transfer process (Brunschwig et al., 1984; Peterson-Kennedy et al., 1984; Simolo et al., 1984). In this case, although multiple intermediates need not be invoked, the relatively small reaction rate constants may again be a consequence of long-distance electron transfer. By extending these investigations to include other structurally defined redox proteins, it may become possible to better define those structural features (distance between chromophores, relative orientations, etc.) which influence the rates of biological electron transfer in protein–protein complexes that are stabilized by electrostatic forces.

Registry No. LFH$^-$ (N^1 anion), 80538-67-6; LFH$^-$ (N^5 anion), 83354-22-7; 5-dRF, 101759-37-9; FNR$_{ox}$, 9029-33-8; cytochrome *c*, 9007-43-6.

REFERENCES

Ahmad, I., Cusanovich, M. A., & Tollin, G. (1982) *Biochemistry 21*, 3122–3128.

Ambler, R. P., Meyer, T. E., Kamen, M. D., Schichman, S. A., & Sawyer, L. (1981) *J. Mol. Biol. 147*, 351–356.

Bartsch, R. G. (1971) *Methods Enzymol. 23*, 344–363.

Bhattacharyya, A. K., Tollin, G., Davis, M., & Edmondson, D. E. (1983) *Biochemistry 22*, 5270–5279.

Bhattacharyya, A. K., Meyer, T. E., & Tollin, G. (1986) *Biochemistry 25*, 4655–4661.

Blankenhorn, G. (1976) *Eur. J. Biochem. 67*, 67–80.

Brunschwig, B. S., Ehrenson, S., & Sutin, N. (1981) *J. Am. Chem. Soc. 106*, 6858–6859.

Cusanovich, M. A., & Tollin, G. (1980) *Biochemistry 19*, 3343–3347.

Cusanovich, M. A., Meyer, T. E., & Tollin, G. (1985) *Biochemistry 24*, 1281–1287.

Draper, R. D., & Ingraham, L. L. (1968) *Arch. Biochem. Biophys. 125*, 802–808.

Dus, K., Sletten, K., & Kamen, M. D. (1968) *J. Biol. Chem. 243*, 5507–5518.

Foust, G. P., Mayhew, S. G., & Massey, V. (1969) *J. Biol. Chem. 244*, 964–970.

Hazzard, J. T., & Tollin, G. (1985) *Biochem. Biophys. Res. Commun. 130*, 1281–1286.

Hazzard, J. T., Cusanovich, M. A., Tainer, J. A., Getzoff, E. D., & Tollin, G. (1986) *Biochemistry 25*, 3318–3328.

Keirns, J. J., & Wang, J. H. (1972) *J. Biol. Chem. 247*, 7374–7382.

Meyer, T. E. (1985) *Biochim. Biophys. Acta 806*, 175–183.

Meyer, T. E., Przysiecki, C. T., Watkins, J. A., Bhattacharyya, A. K., Simondsen, R. P., Cusanovich, M. A., & Tollin, G. (1983) *Proc. Natl. Acad. Sci. U.S.A 80*, 6740–6744.

Peterson-Kennedy, S. E., McGourty, J. L., & Hoffman, B. M. (1984) *J. Am. Chem. Soc. 106*, 5010–5012.

Pettigrew, G. W., Bartsch, R. G., Meyer, T. E., & Kamen, M. D. (1978) *Biochim. Biophys. Acta 503*, 509–523.

Przysiecki, C. T., Bhattacharyya, A. K., Tollin, G., & Cusanovich, M. A. (1985) *J. Biol. Chem. 260*, 1452–1458.

Salemme, F. R., Kraut, J., & Kamen, M. D. (1973) *J. Biol. Chem. 248*, 7701–7706.

Simolo, K. P., McLendon, G. L., Mauk, M. R., & Mauk, G. A. (1984) *J. Am. Chem. Soc. 106*, 5012–5013.

Simondsen, R. P., & Tollin, G. (1983) *Biochemistry 22*, 3008–3016.

Simondsen, R. P., Weber, P. C., Salemme, F. R., & Tollin, G. (1982) *Biochemistry 21*, 6366–6375.

Timkovich, R., & Dickerson, R. E. (1976a) *J. Biol. Chem. 251*, 4033–4046.

Timkovich, R., & Dickerson, R. E. (1976b) *J. Biol. Chem. 251*, 2197–2206.

Tollin, G., Meyer, T. E., & Cusanovich, M. A. (1982) *Biochemistry 21*, 3849–3856.

Tollin, G., Cheddar, G., Watkins, J. A., Meyer, T. E., & Cusanovich, M. A. (1984) *Biochemistry 23*, 6345–6349.

Weber, P. C., & Tollin, G. (1985) *J. Biol. Chem. 260*, 5568–5573.

Zanetti, G., & Curti, B. (1980) *Methods Enzymol. 69*, 250–255.